MATEC Web of Conferences **27**, 02006 (2015)
DOI: 10.1051/matecconf/20152702006

Investigation of the Effects of Solution Temperature on the Corrosion Behavior of Austenitic Low-Nickel Stainless Steels in Citric Acid using Impedance and Polarization Measurements

Francis M. Mulimbayan[1, a] and Manolo G. Mena[2, b]

[1] *Department of Engineering Science, University of the Philippines Los Baños, Philippines*
[2] *Department of Metallurgical, Mining and Materials Engineering, University of the Philippines – Diliman, Philippines*

Abstract. Stainless steels may be classified according to alloy microstructure – ferritic, austenitic, martensitic, duplex, and precipitation hardening grades. Among these, austenitic grade has the largest contribution to market due to the alloy's numerous industrial and domestic applications. In this study, the corrosion behavior of low-Nickel stainless steel in citric acid was investigated using potentiodynamic polarization techniques and Electrochemical Impedance Spectroscopy (EIS). The corrosion current density which is directly related to corrosion rate was extracted from the generated anodic polarization curve. Increasing the temperature of the citric acid resulted to increased corrosion current densities indicating higher corrosion rates at initial corrosion condition. EIS was performed to generate Nyquist plots whose shape and size depicts the corrosion mechanism and corrosion resistance of the alloy in citric acid, respectively. All the generated Nyquist plots have depressed semi-circle shapes implying that corrosion process takes place with charge-transfer as the rate-determining step. Based from the extracted values of polarization resistance (Rp), the temperature of the solution has negative correlation with the corrosion resistance of the studied alloy.

1 Introduction

Stainless steel (SS) is used in numerous industrial and domestic applications worldwide [1]. It is even used as orthopedic implant materials for fracture and joint replacement [2]. The world production of stainless steel has already reached 32.1 Mt in year 2011 and the rate of production continuously increases. SS is best-known for having notable corrosion resistance that is attributed to alloy's chromium (Cr) content [3]. SS may be classified based on its microstructure – ferritic, austenitic, duplex, martensitic, and precipitation hardening grades. Ferritic SS has a ferrite as its stable phase while in the case of austenitic SS, austenite phase exists [1, 4]. Duplex has roughly 50% ferritic and 50% austenitic. Martensitic grades have higher carbon (C) content and produced by rapidly cooling the SS after being brought to austenitizing temperature [1]. Finally, precipitation hardening grades are developed for applications requiring high tensile strengths [5]. The American Iron and Steel Institute (AISI) used three-digit numbering system for SS. It consists of a 300-series for chromium-nickel (Cr-Ni) austenitic alloys, a 400-series for high-Cr ferritic and martensitic alloys, a 200-series for austenitic low-Nickel alloys, a 500-series for 4-6% Cr alloys and a 600-series to cover proprietary alloys [6]. Between the two austenitic grades – AISI 200 and 300-series, it is the latter alloy which is commonly produced in applications involving food handling and processing, though the use of former alloy has increased considerably due to continuous effort of cutting cost that is achieved by significantly reducing the amount of nickel and using manganese instead.

Citric acid in food industries is usually dissolved beforehand creating an acidic aqueous solution. It provides a corrosive environment to the tanks, pipes, container, chemical plant components and food contact equipment exposed to it [7]. In this study, the corrosion behavior of AISI 202 – a low-Ni stainless steel, was investigated in citric acid media with varying temperatures (ambient, 50ºC and 70ºC) using Potentiodynamic Polarization and Electrochemical Impedance Spectroscopy.

2 Methodology

Specimens of AISI 202 stainless steel (SS) with test area of roughly 0.25 cm^2 were cut and mounted in quick-setting resin. Electrical connection was made to each specimen before mounting. This was done by soldering copper wire on the reverse side of each specimen. The wire was insulated using 4-mm-diameter glass tubes to avoid contact with the solution. Mounting of epoxy was done in such a way that only the test area was exposed to the solution. The test area of each sample was mechanically polished using series of SiC paper. After

Corresponding author: [a] fmmulimbayan@gmail.com; [b] lito.mena@nxp.com.

polishing, it was then rinsed with running water, ultrasonically cleaned with distilled water and immediately inserted to the test cell with maximum delay of 30 minutes. Prior to electrochemical testing, the chemical composition of the investigated alloys was determined using Optical emission Spectroscopy (OES). Precise amounts of reagent grade citric acid monohydrate were weighed using analytical balance (Shimadzu) and dissolved in commercially available distilled water then shook thoroughly in a 500 mL volumetric flask to make appropriate test solutions.

Experiments were carried out using a conventional three-electrode cell assembly with 1 cm x 1 cm counter electrode (CE) made of Platinum (Pt) and Ag/AgCl reference electrode (RE) with Luggin capillary. EIS and potentiodynamic polarization were carried out using a computer-controlled potentiostat (AUTOLAB PGSTAT128N METROHM) in tandem with NOVA software. EIS measurements were performed at open-circuit potential in the frequency range 100 kHz to 0.01 Hz with perturbation signal of 5 mV rms. Based from the generated Nyquist plots, the corresponding equivalent circuit which describes the behavior of the electrode-electrolyte system was determined. Potentiodynamic polarizations were achieved at a scan rate of 0.3mV/s in the applied range of -600 up to +200 mV. All the measured potential values were quoted with respect to Ag/AgCl RE.

3 Results and discussion

3.1 Potentiodynamic polarization

Polarization plot displays the variation of applied potential (E) against the logarithm of current density (log i). The polarization curve of all alloys showing an active-passive behavior like SS can be divided into three potential domains, namely (1) cathodic, (2) anodic-cathodic transition and (3) anodic region. The third domain which lies above the corrosion potential (E_{corr}) can be further divided into three parts – active, passive and transpassive region [8]. Given the potentiodynamic polarization curves, the corrosion current density (i_{corr}) and E_{corr} can be determined using Tafel extrapolation. This technique requires extending the linear portions of both anodic and cathodic Tafel regions of the polarization curves and the intersection corresponds to the values of E_{corr} and i_{corr}. The linear portions however, should extend over one decade on the log-i axis – a feature which is only partially satisfied by SSs and other alloys with active-passive behavior. The polarization curves of these alloys have no well-defined anodic Tafel regions and thus, i_{corr} based on the intersection of anodic and cathodic Tafel line at the E_{corr} will only lead to erroneous values [9]. Given that the cathodic polarization curves exhibit wide and well-defined Tafel regions, estimation of i_{corr} was made by extrapolation of the cathodic Tafel lines back to the corresponding values of E_{corr}. If E_{corr} denotes the potential of the alloy at initial corrosion condition, i_{corr} on the other hand, corresponds to the initial corrosion current density. While more positive E_{corr} indicates greater stability, higher i_{corr} means higher initial corrosion rate of the alloy in a designated aqueous media.

The influence of solution temperature on the corrosion behavior of AISI 202 stainless steel is evident in Fig.1. Blue, green and red lines represent the polarization scans at 23±0.5ºC, 50ºC and 70ºC, respectively. Temperature greatly affects corrosion process since corrosion is an electrochemical reaction, and reaction rates increase with increasing temperature. As temperature is increased from 23±0.5ºC to 50ºC, the cathodic arm of the polarization curve shifted in the direction of higher current densities and raising the temperature further from 50 to 70ºC only produces small effects as indicated by nearly overlapping red and green cathodic arms. This indicates that upon increasing the temperature, the rate of H_2 evolution reaction increases and eventually reaches a maximum value. In this condition, the position of cathodic arm will be fixed and shifting to higher corrosion currents may no longer occur.

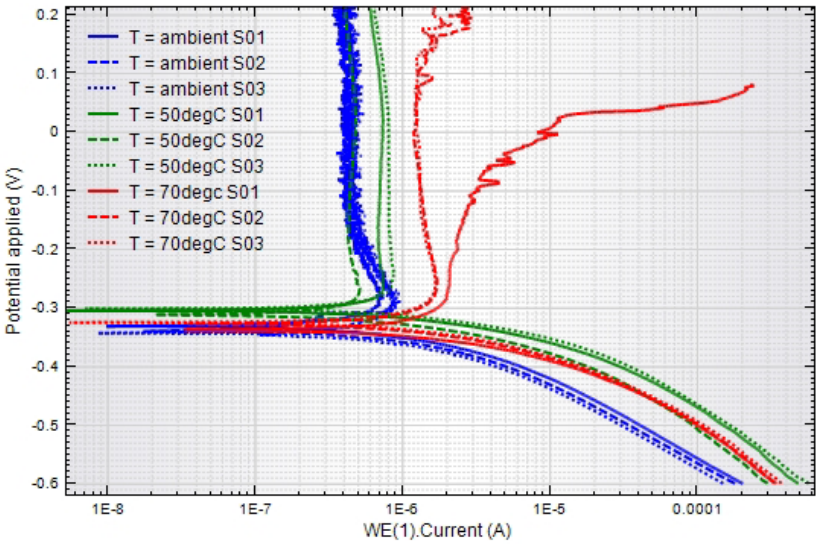

Figure 1. Potentiodynamic polarization curves of AISI 202 SS in N2-purged citric acid at 100 g/L

Corrosion current densities (i_{corr}) were extracted from polarization curves in Fig. 1, averaged, and plotted as a function of citric acid temperatures as shown in Fig. 2a. It can be deduced that the corrosion rate increases with increasing solution temperature. This observed increase in i_{corr} values may be attributed to the alloy's increased tendency to undergo dissolution process at elevated temperatures. Values of corrosion potential (E_{corr}) were also determined from Fig. 1. The average of the three replicates were computed and plotted as function of acid's temperature as shown in Fig. 2b. Initial rise in E_{corr} is observed upon raising the citric acid temperature from 23±0.5ºC to 50ºC and exhibited subsequent drop in E_{corr} by further increasing the temperature from 50 to 70ºC. The alloy's response from 23±0.5 to 50ºC is in contrast to what is anticipated since higher temperature typically increases the aggressiveness of the corrosive media favoring dissolution of alloy components. This may imply that increased solution temperature resulted to higher tendency of forming an oxide layer but further thickening of this film becomes less favorable due to high dissolution rate.

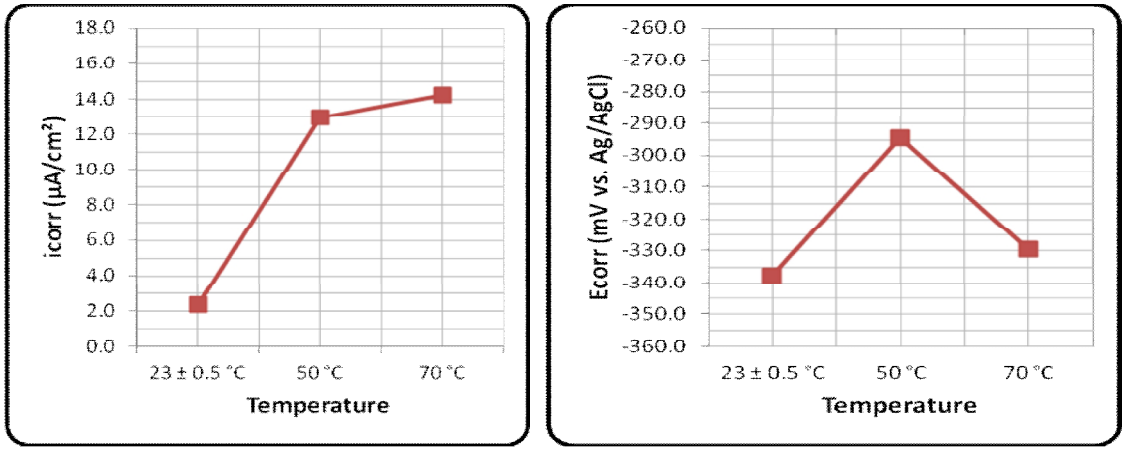

(a) (b)

Figure 2. Plot of average (a) Ecorr and (b) icorr against solution temperature of austenitic low-Ni stainless steel in N2-purged citric acid at 100 g/L concentration

3.2 Electrochemical impedance spectroscopy

In potentiodynamic polarization, the electrode reactions are investigated through the application of large perturbations on the studied electrochemical system in which electrode is driven away from the equilibrium by imposing potential sweeps. EIS, on the other hand, involves application of small sinusoidal potentials that will result to sinusoidal currents. This electrochemical technique which is performed in open circuit condition is known to induce no significant disturbance on the properties being measured [10, 11]. In this technique, the polarization resistance (R_p) of a metallic specimen can be determined by measuring the electrochemical impedance made at a series of predetermined frequencies [12]. EIS data is commonly analyzed by fitting it to an equivalent electrical circuit (EC) model of the interface.

Nyquist plots illustrating the effects of solution temperature on the corrosion resistance are shown in Fig. 3a. The blue, green and red loops correspond to impedance measurements at 23±0.5, 50 and 70ºC, respectively. The size of these impedance loops represents the resistance of the studied alloy to polarization, and thus to corrosion. The alloy at 23±0.5ºC exhibited capacitive loops with largest diameter, and thus the highest R_p. The size of the capacitive loops decreases as solution temperature increases indicating higher corrosion rate at elevated temperatures. This inverse dependence of corrosion resistance on the solution temperature becomes even more apparent by plotting the average R_p obtained from EC fitting against the solution temperature as illustrated in Fig. 3b. The results obtained from EIS are in agreement with that of i_{corr} measurements.

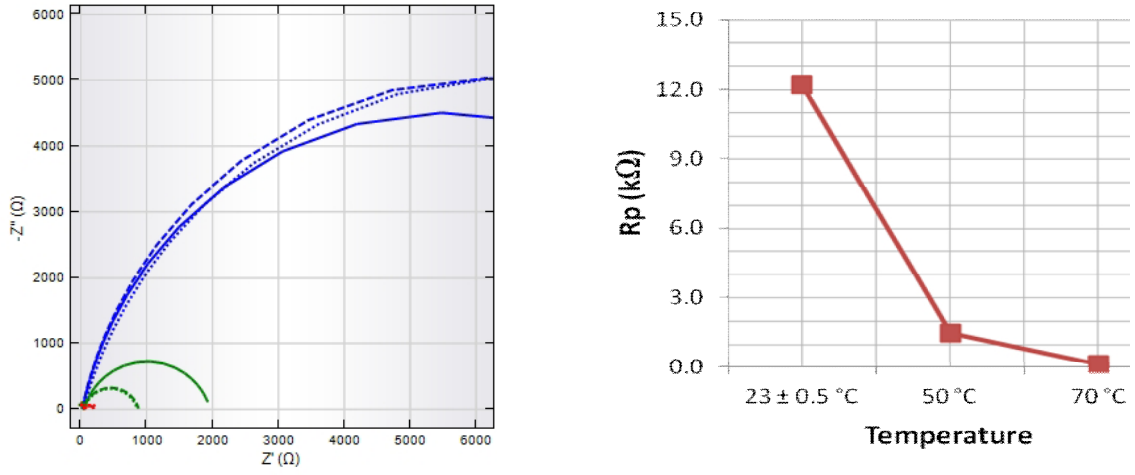

(a) (b)

Figure 3. (a) Nyquist plots of low-Ni stainless steels in citric acid at 100 g/L; blue, green and red loops correspond to impedance measurements at 23, 50 and 70ºC, respectively; (b) Plot of average Rp vs. solution temperature of low-Ni SS in N2-purged citric acid

The generated Nyquist plots for all the studied temperatures, as also depicted in Fig. 3 appear as depressed semi-circles (or capacitive loops) indicating that corrosion process is charge-transfer controlled. This depression of capacitive loops may be attributed to surface heterogeneities [9].

4 Summary and Conclusions

An electrochemical investigation was performed on AISI 202 SS – a low-Ni, austenitic Cr-Mn SS, in order to evaluate its corrosion behavior in 100 g/L citric acid concentration subjected to different temperatures (23±0.5, 50 and 70ºC). Electrochemical techniques such as potentiodynamic polarization and EIS were used to extract information regarding the stability and corrosion rate of the studied alloy in the designated environment. Increased solution temperature resulted to increased i_{corr} implying increased corrosion rate at initial corrosion condition. The R_p values extracted from impedance spectra are observed to have negative correlation with temperature suggesting that corrosion resistance decreases with increasing temperature.

Acknowledgement

This work was financially supported by ERDT. Also, I would like to thank Dr. Manolo G. Mena for sharing his expertise to make this study possible. Finally, I acknowledge DMMME for the use of potentiostat and allowing me to work in Smart and Functional Laboratory.

References

1. P. A. Schweitzer, Corrosion Engineering Handbook (Marcel Dekker, Inc, USA 1996)
2. C. Ornhagen, J. O. Nilsson and H. Vannevik, Characterization of a Nitrogen-rich Austenitic Stainless Steel used for Osteosynthesis Devices (Biomedical Material Research, **31**(1), pp. 97-103, (1996)
3. M. Kemp, A. Van Bennekom and F. P. A. Robinson, Evaluation of the Corrosion and Mechanical Properties of Experimental Cr-Mn Stainless Steels (Materials Science and Engineering, pp. 183-194, (1995).
4. Information on http://www.assda.asn.au/images/stories/oldcontent/19673001161232771640.pdf.
5. Information on www. atlassteels.com.au.
6. H. M. Cobb, The Naming and Numbering of Stainless Steels, Advanced Materials & Processes **165**, pp. 39-44, (2007).
7. C. R. Soccol. L. P. S. Vandenberghe and C. Rodrigues, New Perspectives for Citric Acid Production and Application (Food Technology and Biotechnology, **44**, pp. 141-149, (2006).
8. M. Saadawy, Kinetic of Pitting Dissolution of Austenitic Stainless Steel 304 in Sodium Chloride Solution (ISRN Corrosion, **2012**, pp. 1-5, 2012)
9. A. A. Hermas and M. S.Morad, A Comparative study on the Corrosion Behavior of 304 Austenitic Stainless Steel in Sulfamic and Sulfuric Acid Solutions (Corrosion Science, **50**, pp. 2710-2717, 2008)
10. A. J. Bard, L. R. Faulkner, E. Swain and C. Robey, Electrochemical Methods. Fundamentals and Applications. 2nd ed. (John Wiley & Sons, Inc., 2001)
11. GAMRY Instruments Inc.: Application Notes on Basic of Electrochemical Impedance Spectroscopy (1990)
12. P. Marcus and F. Mansfeld: Analytical Methods in Corrosion Science and Engineering (CRC Taylor & Francis, 2006)